Effective Interactions between Polyhedral Oligomeric Sislesquioxanes Dissolved in Normal Hexadecane from Molecular Simulation

Alberto Striolo,* Clare McCabe, and Peter T. Cummings

Department of Chemical Engineering, Vanderbilt University, Nashville, Tennessee 37235

Received June 18, 2005; Revised Manuscript Received August 16, 2005

ABSTRACT: Polyhedral oligomeric silsesquioxanes show promising applications as organic−inorganic nanocomposite building blocks that can be used, for example, to enhance the properties of polymeric materials. In this work radial distribution functions, potentials of mean force, and self-diffusion coefficients are obtained from molecular dynamics simulations for polyhedral oligomeric silsesquioxane (POSS) monomers dissolved in normal hexadecane in the temperature range 400−1000 K. The calculated potentials of mean force show a marked dependence on temperature and on the organic substituents tethered to the silsesquioxane cages. Selected simulation snapshots are used to elucidate the mechanism by which two POSS monomers approach each other. The results obtained are compared to calculations for the potentials of mean force between POSS monomers dissolved in poly(dimethylsiloxane) reported in earlier work [Striolo, A.; McCabe, C.; Cummings, P. T. *J. Phys. Chem. B* **2005**, *109*, 14300]. Additionally, from the simulated potentials of mean force we calculate osmotic second virial coefficients as a function of temperature. Our results indicate that in both hexadecane and poly(dimethylsiloxane) the osmotic second virial coefficient is negative for $Si_8O_{12}H_8$ monomers at all temperatures considered, while that for $Si_8O_{12}(CH_3)_8$ monomers is negative at low temperatures and becomes positive as the temperature increases. The theta temperature (i.e., the temperature at which the osmotic second virial coefficient equals zero) is approximately 550 and 700 K for $Si_8O_{12}(CH_3)_8$ in poly(dimethylsiloxane) and in normal hexadecane, respectively.

1. Introduction

The mechanical properties of synthetic polymeric materials can often be improved by the incorporation of nanoscale particulates.[1−4] Polyhedral oligomeric silsesquioxanes (POSS)[5] attract significant interest as nanoscale building blocks for synthesizing nanocomposite materials (e.g., POSS molecules functionalized with polymer, cross-linked, and alloyed with a polymer matrix). POSS molecules are cages of silicon and oxygen having the chemical formula $Si_8O_{12}R_8$, where R is an organic group. A schematic representation of one POSS monomer, $Si_8O_{12}H_8$, in which R is one hydrogen atom, is provided in Figure 1. POSS chemistry is extremely flexible; alcohols, chlorosilanes, epoxides, esters, isocyanates, acrylates, silanes, etc.,[6] have been substituted onto the POSS cage. This flexibility suggests a wide range of potential applications for POSS-based nanocomposites.[7−9]

POSS monomers have been incorporated as fillers in several polymers, including methacrylates, siloxanes, styryls, and poly(propylene).[10,11] The zero-shear-rate viscosity of a polymer can be tuned by adding POSS monomers as fillers. At low loading (10−20 wt % POSS) the POSS monomers are well dispersed in the polymeric matrix, and the viscosity of the filled polymer decreases; as the loading increases (above 20−30 wt % POSS), the POSS monomers form crystallites and the viscosity of the system increases in a way consistent with classical predictions for hard-sphere suspensions.[11] To promote uniform dispersions in the material, it is convenient to chemically bind small amounts of POSS monomers to the polymer chains.[12−14] Enhanced properties of POSS-based hybrid copolymers include increased thermal stability, higher glass transition temperatures, increased flame and heat resistance, and enhancement in the modulus and melt strengths.[15]

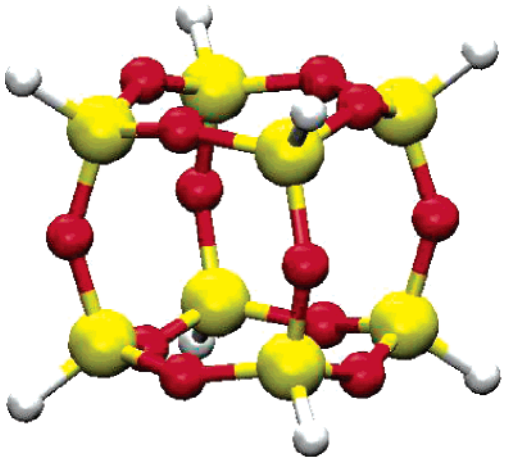

Figure 1. Schematic representation of one POSS monomer of chemical composition $Si_8O_{12}H_8$. Yellow, red, and white spheres represent silicon, oxygen, and hydrogen atoms, respectively. In the octafunctionalized POSS monomer considered in this work $[Si_8O_{12}(CH_3)_8]$ the hydrogen atoms are substituted by methyl groups.

Despite the large body of experimental work on POSS−polymer systems, neither the microstructure of the copolymers nor the mechanism of reinforcement is well understood. The changes in thermodynamic and mechanical behavior can be attributed to the size of the POSS monomer, the nature of the organic periphery, the number of reactive functionalities, the concentration and solubility of POSS monomers in the material, etc. These and other factors determine whether POSS

* To whom all correspondence should be addressed. Current address: University of Oklahoma, School of Chemical Biological and Materials Engineering 100 East Boyd, Sarkeys Energy Center Room T-235, Norman, OK 73019. Ph 1 405 325 5716, Fax 1 405 325 5813, e-mail astriolo@ou.edu.

10.1021/ma0512859 CCC: $30.25
Published on Web 09/22/2005

monomers are incorporated as isolated and uniformly dispersed molecules, isolated phase-separated particles, or matrix-bound aggregates.[13,14] Understanding and controlling the nanostructure of polymers containing silsesquioxanes will enable us to design materials with tailored properties for selected applications.[16] In this scenario, molecular simulations provide useful insights.[17−19] For example, we recently reported simulation results for the potential of mean force and for the diffusion coefficients of POSS monomers dissolved in a melt of short poly(dimethylsiloxane) chains (PDMS).[20] The POSS monomers we considered were $Si_8O_{12}H_8$ and $Si_8O_{12}(CH_3)_8$. Our results demonstrated that by substituting the organic group R on the POSS cage it is possible to significantly alter the features of the pair potential of mean force between POSS monomers. In particular, we showed that the potential of mean force between $Si_8O_{12}H_8$ monomers dissolved in PDMS is in general significantly more attractive than that between $Si_8O_{12}(CH_3)_8$. We also observed that the motion of dissolved POSS monomers could be characterized by a hopping mechanism.

In the current work we are interested in understanding the effects of the chemistry of the polymeric solvent on the thermodynamic and transport properties of dissolved POSS monomers. To this end we dissolve the silsesquioxanes in a melt of normal hexadecane (nC_{16}) and compare the results to those obtained for silsesquioxanes in PDMS. The number of repeating units in one hexadecane molecule (16) is equal to the number of monomers in the PDMS chains used in our previous work,[20] and the system density is $\sim$0.8 g/cm^3, as in our earlier work. The density chosen for our simulations is similar to the specific gravity of nC_{16} at room temperature (0.773). Several differences can be identified between nC_{16} and PDMS. The monomers that constitute nC_{16} chains are less bulky than those that constitute PDMS chains; nC_{16} freezes at temperatures close to room temperature, while PDMS is a rubbery polymer in the temperature range 300−1000 K. Because of inherent limitations in the algorithms used within molecular dynamics, we cannot explore thermodynamic conditions that are close to the solid state for nC_{16}; thus, we restrict our study to the temperature range 400−1000 K. As in our earlier simulations, we concentrate on studying the properties of two representative POSS monomers. The first consists of bare POSS ($Si_8O_{12}H_8$) while the second consists of octafunctionalized POSS in which the hydrogen atoms are substituted by methyl groups [$Si_8O_{12}(CH_3)_8$]. Normal hexadecane is chemically different from $Si_8O_{12}H_8$, but we expect it to be compatible with $Si_8O_{12}(CH_3)_8$. While POSS monomers, as well as normal hexadecane, probably decompose at 1000 K (the boiling point of nC_{16} is 560 K, and pyrolysis data have been reported in the temperature range 673−723 K),[21] our hypothetical results at 1000 K correspond to what would be obtained in the absence of decomposition. These simulations are representative of a thought experiment in which the temperature is raised for a short period of time, not sufficient for the materials to decompose, but long enough to promote fast thermal motion in the system.

The remainder of this paper is organized as follows: in section II we present the simulation method and details of the force fields used; in section III we discuss our results for the effective pair potential of mean force between POSS monomers and their diffusion coefficients when dissolved in normal hexadecane at 400, 600, and 1000 K. From the simulated pair potentials of mean force we compute the osmotic second virial coefficients for pair of POSS monomers dissolved in nC_{16} and in PDMS as a function of temperature. In the last section of this paper we summarize our conclusions.

2. Simulation Details

Force Fields. POSS monomers are described by implementing a force field originally developed to reproduce the radial distribution function of liquid PDMS.[22] In this work the hydrogen atoms in the bare POSS monomer are not involved in dispersive interactions but are included in the calculation of short-range potentials (bond stretch, bond angle, and torsional constraints) that determine the structure of the POSS cage. The methyl groups in the POSS monomers are treated with a united-atom approach according to the TraPPE force field.[23]

Atoms in the same POSS monomer interact with each other via short-range potentials that account for bond length, bond angles, and torsional constraints. Bond-length fluctuations around the equilibrium separation r_0 are subject to harmonic functional forms:

$$V_b(r) = k_b(r - r_0)^2 \tag{1}$$

Similarly, bond angle oscillations about the equilibrium angle θ_0 are subject to harmonic constraints:

$$V_a(\theta) = k_a(\theta - \theta_0)^2 \tag{2}$$

Torsional angle fluctuations ϕ are subject to torsional potentials with functional form

$$V_t(\phi) = c_1[1 + \cos(\phi)] + c_2[1 - \cos(2\phi)] + c_3[1 + \cos(3\phi)] \tag{3}$$

In eqs 1−3 V_b, V_a, and V_t are the bond, angle, and torsional potentials, respectively; k_b, k_a, c_1, c_2, and c_3 are proportionality constants; r, θ, and ϕ are the instantaneous bond length, bond angle, and torsional angle, respectively.

In addition to intramolecular forces, Lennard-Jones 12−6 potentials describe nonbonded CH_3-CH_3, CH_3-O, and CH_3-Si dispersive interactions:

$$u(r_{ij}) = 4\epsilon_{ij}\left[\left(\frac{\sigma_{ij}}{r_{ij}}\right)^{12} - \left(\frac{\sigma_{ij}}{r_{ij}}\right)^{6}\right] \tag{4}$$

Lennard-Jones 9−6 potentials describe nonbonded Si−O dispersive interactions:

$$u(r_{ij}) = \epsilon_{ij}\left[2\left(\frac{\sigma_{ij}}{r_{ij}}\right)^{9} - 3\left(\frac{\sigma_{ij}}{r_{ij}}\right)^{6}\right] \tag{5}$$

In eqs 4 and 5 the parameters ϵ_{ij} and σ_{ij} have the usual meaning; r_{ij} is the distance between atoms i and j. Nonbonded interactions between atoms in the same molecule are not accounted for unless the pairs of atoms are separated by more than three bonds, consistent with many formalisms including the TraPPE force field.[23] We recognize that the use of the 12−6 formalism to describe nonbonded CH_3-CH_3, CH_3-O, and CH_3-Si dispersive interactions is not consistent with the use of the 9−6 formalism to describe the nonbonded Si−O dispersive interactions. This is a result of the different functional

Table 1. Potential Parameters for the Molecular Models Employed in This Work

bonds	r_0/Å	k_b/kcal/(mol Å^2)
Si−O	1.64	350.12
Si−CH_3	1.90	189.65
angles	θ_0/deg	k_θ/kcal/(mol rad^2)
Si−O−Si	146.46	14.14
O−Si−O	107.82	94.50
O−Si−CH_3	110.69	49.97
CH_3−CH_2−CH_2	114.00	62.09
CH_2−CH_2−CH_2	114.00	62.09
dihedrals	c_1/kcal/mol	c_2/kcal/mol	c_3/kcal/mol
Si−O−Si−O	0.2250	0.0000	0.0000
Si−O−Si−CH_3	0.0000	0.0000	0.0100
CH_3−CH_2−CH_2−CH_2	0.7054	−0.1355	1.5724
CH_2−CH_2−CH_2−CH_2	0.7054	−0.1355	1.5724
nonbonded interactions	σ_{ij}/Å	ϵ_{ij}/kcal/mol
Si−Si	4.29	0.1310
O−O	3.30	0.0800
Si−O	3.94	0.0772
CH_3−CH_3	3.75	0.1947
CH_2−CH_2	3.95	0.0974
CH_3−CH_2	3.85	0.1377
Si−CH_3	3.83	0.1596
Si−CH_2	3.93	0.1093
O−CH_3	3.38	0.1247
O−CH_2	3.48	0.0854

forms for the nonbonded interactions in the force fields for silsesquioxanes and for alkanes. In this work we implement the force fields as they were originally derived, and we use the method of Frischknecht and Curro[22] to address the treatment of cross interactions. In a forthcoming paper[24] we compare predictions for melting temperature and crystal structure of POSS crystals using several different force fields. In that work we conclude that the force field used here offers a good compromise between reliability and economy of computational time. However, we have not attempted to evaluate systematically the effect of uncertainties in the force fields on the calculated properties.

Normal hexadecane is simulated by implementing the TraPPE force field for alkanes.[23] CH_3 and CH_2 groups in the hydrocarbon chain are treated as united atoms, and the hydrogen atoms are not treated explicitly. The united atoms are linked through rigid bonds of length 0.154 nm. The fluctuations of bond angles and of dihedral angles are constrained through harmonic potentials of functional form analogous to those expressed by eqs 2 and 3.

Nonbonded interactions between united atoms are treated within the Lennard-Jones 12−6 formalism, reported in eq 4. Interactions between dissimilar united atoms are described via Lennard-Jones 12−6 potentials where the interaction parameters are obtained from the interaction parameters of the similar united atoms through the Lorentz−Berthelot mixing rules. Nonbonded interactions between atoms in the same molecule are not accounted for unless the pairs of atoms are separated by more than three bonds.

Nonbonded interactions between atoms belonging to POSS and nC_{16} are treated according to the Lennard-Jones 12−6 formalism expressed in eq 4 with the appropriate choice of interaction parameters.

In Table 1 we report the parameters required to implement the force fields used here to describe POSS monomers and nC_{16} chains.

Simulation Algorithm. Classical molecular dynamics simulations are employed to study the properties of systems containing POSS monomers and nC_{16}. The systems considered are composed of five POSS monomers and 122 nC_{16} chains diluted in a cubic simulation box of size 4.0 nm. The total number of nC_{16} molecules is chosen to achieve a total density in the systems of ~0.8 g/cm^3. The simulation box size is adequate for the purposes of our studies, as discussed elsewhere.[20]

To integrate the equations of motion, we employ the DL-POLY (version 2.14) simulation suite[25] in the canonical (*NVT*) ensemble.[26] The temperature is controlled using the Nosé-Hoover thermostat (time constant between 0.5 and 2 ps). The integration time is 1 fs at 400 K and 0.5 fs at higher temperatures. Rigid bonds are maintained using the SHAKE algorithm.[27] The initial configurations are obtained using a Monte Carlo procedure developed to study colloid−polymer systems;[28] the POSS monomers are placed in the simulation box with one molecule located in the box center and the other four along the box main diagonals. The nC_{16} chains are then grown within the simulation box using periodic boundary conditions in all directions. The building subroutine solely ensures that the connectivity between different polymer segments is respected and that different polymer segments do not overlap either with each other or with the POSS monomers. The complete interatomic potentials are switched on in the subsequent simulation phases. The initial configurations are relaxed at elevated temperatures (1000 K) for 500 ps. Relaxed configurations are then brought abruptly to the temperatures of interest, and at each temperature the first 500 ps of simulation data are discarded to allow for complete equilibration. During the equilibration phase, the velocities are rescaled every 2000 time steps. The equilibration is considered sufficient when the total energy reaches a plateau. The production phase lasts 4 ns at each temperature considered. No drift in the total energy is observed during the production phase. One system configuration is stored every 500 fs. These configurations are used to compute the radial distribution function between the centers of mass of the POSS monomers and the self-diffusion coefficients. From the radial distribution function the effective potential of mean force between pairs of POSS monomers is computed according to[29]

$$\frac{W(r)}{kT} = -\ln[g(r)] \tag{6}$$

In eq 6 $W(r)$ and $g(r)$ are the potential of mean force and the radial distribution function at a separation r between the centers of mass of two POSS monomers, respectively; k is the Boltzmann constant and T is the absolute temperature. All the radial distribution functions reported in this work were computed between the centers of mass of the POSS monomers. While $g(r)$ depends on the relative orientation of the POSS monomers, in our calculations we do not differentiate results obtained at different POSS−POSS relative orientations, and therefore we consider our results as an orientation-averaged radial distribution function. The most favorable POSS−POSS orientations will simply occur more often during the course of the simulation, and therefore their contribution will be more significant than that of least-favorable POSS−POSS relative orientations. To ensure reliability of the results, we repeat the simulations at least five times for each system. Therefore, the

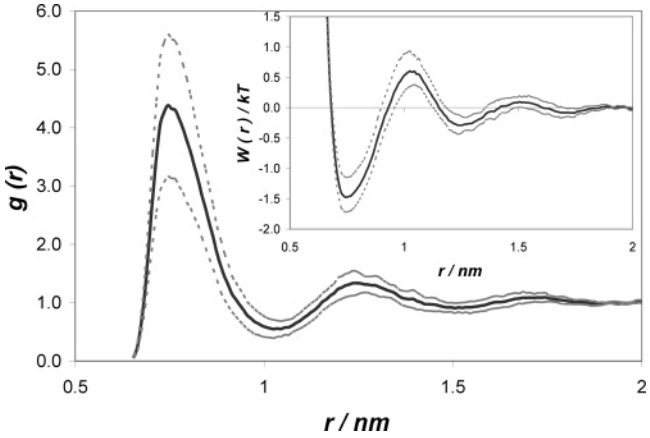

Figure 2. Radial distribution function and effective pair potential of mean force (inset) between bare POSS monomers dissolved in nC_{16} as a function of the distance between centers of mass of the POSS monomers. Results are reported for T = 400 K (black solid line). The gray dotted lines delimit the statistical uncertainties of the results reported.

total production time was of at least 20 ns for each temperature considered. At low temperatures longer simulation runs are required.

From the effective pair potential of mean force between macromolecules in solution it is possible to compute the osmotic second virial coefficient, B_{22}, according to[29]

$$B_{22} = 2\pi \int_0^\infty r^2 \left\{ 1 - \exp\left[\frac{-W(r)}{kT} \right] \right\} \mathrm{d}r \qquad (7)$$

The osmotic second virial coefficient is an experimentally accessible quantity (see, for example, ref 30 and references therein), and it provides macroscopic evidence of effective interactions between macromolecules. When B_{22} is positive, the effective molecule−molecule interactions are repulsive. When B_{22} is negative, the effective molecule−molecule interactions are attractive.

To determine the diffusion coefficient D, we compute the mean-square displacement, ΔR^2, of the centers of mass of the POSS monomers as a function of time and fit the simulation results to the Einstein equation:

$$D = \frac{1}{6} \lim_{t \to \infty} \frac{\Delta R^2}{\mathrm{d}t} \qquad (8)$$

To construct the mean-square displacement, we consider 20 origins separated by 150 ps and average over the trajectories recorded for the five POSS monomers present in the system. In what follows we report the average diffusion coefficients obtained in our simulations.

Because we conduct our simulation in the NVT ensemble, the pressure increases as the simulation temperature increases. The density chosen guarantees that at room temperature the pressure is approximately atmospheric, but it increases to approximately 0.2 kbar at 400 K, 1.5 kbar at 600 K, and 3.5 kbar at 1000 K. In our discussion for the theta temperature we neglect pressure effects on the osmotic second virial coefficient.

3. Results and Discussion

Radial Distribution Functions and Potentials of Mean Force. In Figure 2 we report the radial distribution function and the potential of mean force (inset) for bare POSS monomers in nC_{16} at 400 K. The black solid lines represent the average results. The limit of uncertainty is delimited by the gray dotted lines, obtained by adding and subtracting the standard deviation to the average at every center-to-center separation. Even though the system simulated is fairly complicated and characterized by long relaxation times (see results for the diffusion coefficients), the results presented in this work are reproducible. (The uncertainty corresponding to the first attractive peak in the potential of mean force is about $0.25kT$ and is larger than that observed at all other center-to-center separations.) Results obtained at higher temperatures are characterized by lower uncertainty because the relaxation time decreases as the temperature increases, and therefore statistical sampling improves.

The results shown in Figure 2 indicate a strong short-range attraction between bare POSS monomers in nC_{16}. The first attractive peak in the radial distribution function (and correspondingly the first attractive peak in the potential of mean force), located at $r \cong 0.75$ nm, is followed by a significant midrange repulsion that corresponds to $\sim 0.6kT$ at $r \cong 1.05$ nm. Because of the small size of the nC_{16} monomers, it is likely that this midrange repulsion is due to the presence of nC_{16} chains in the region that separates two approaching POSS monomers, as was previously observed for the effective pair interaction between spherical colloids dissolved in solutions containing nonadsorbing polymers.[28] Our results for the radial distribution function and for the potential of mean force indicate that the effective POSS−POSS interactions are long-ranged, and a sequence of attractive/repulsive peaks can be observed as far as a center-to-center separation of ~1.75 nm.

To appreciate whether the results discussed in this work depend on the concentration of silsesquioxane monomers in the simulation box, we perform selected simulations with two POSS monomers dissolved within the simulation box and compare the results with those obtained for five POSS monomers in the simulation box. We maintain the number density of nC_{16} chains equal to that considered in the other cases (122 chains); thus, the total density of the system is somewhat lower than that considered in the rest of this work. In Figure 3 we report the radial distribution function for bare (Figure 3A) and octamethylsilsesquioxane monomers (Figure 3B) dissolved in nC_{16} when either two (black dotted lines) or five (black solid lines) monomers are dissolved in the simulation box. When bare POSS monomers are considered (Figure 3A), our results are not distinguishable in the two cases. When octamethyl-POSS are considered, the radial distribution function obtained when two POSS monomers are dissolved in the simulation box (black dotted line) maintains the features of that obtained when five POSS monomers are dissolved in the simulation box (black continuous line), but the first attractive peak is less intense. However, we note that the results obtained when two octamethyl-POSS are dissolved in the system are within the statistical uncertainty of the results obtained when five octamethyl-POSS are considered. Therefore, for both bare and octamethylsilsesquioxanes the radial distribution function at dilute concentrations (less than five POSS monomers in the simulation box), and consequently the pair potential of mean force, does not depend appreciably on the number density of POSS monomers. Because the statistical uncertainty is much larger when only two POSS monomers are dissolved in the simula-

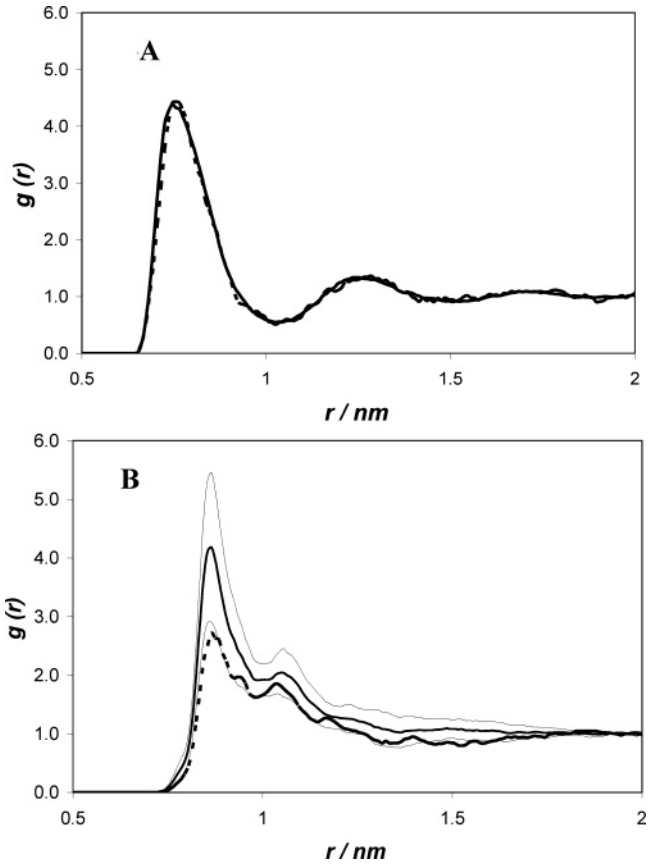

Figure 3. Radial distribution function for POSS monomers dissolved in nC_{16} at $T = 400$ K: (A) bare POSS; (B) octamethyl-POSS. Black continuous lines are for results obtained when five POSS monomers are dissolved in the simulation box; black dotted lines are for results obtained when two POSS monomers are in the simulation box. The gray continuous lines in (B) indicate the statistical uncertainty relative to the calculation of the radial distribution function when five octamethyl-POSS monomers are dissolved in the simulation box.

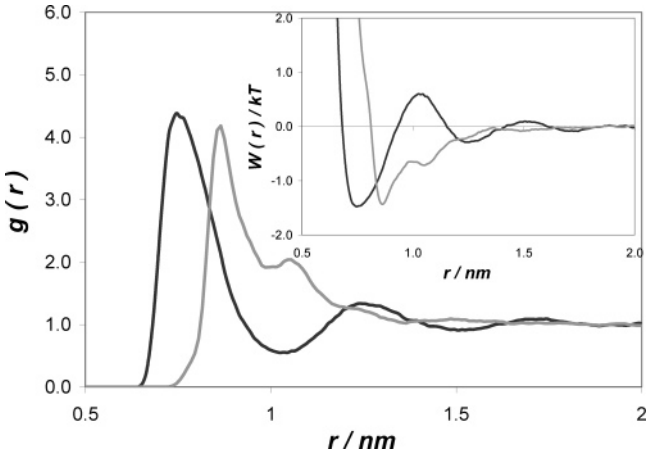

Figure 4. Radial distribution function and effective pair potential of mean force (inset) between POSS monomers dissolved in nC_{16} at $T = 400$ *K*. Black solid lines are for bare POSS ($Si_8O_{12}H_8$). Gray solid lines are for octamethyl-POSS [$Si_8O_{12}(CH_3)_8$]. Statistical uncertainties are not reported for clarity.

tion box, in the remainder of the work we consider five POSS monomers.

In Figure 4 we compare the radial distribution function and the potential of mean force (inset) between bare silsesquioxane cages, $Si_8O_{12}H_8$ (black solid lines), and between octamethyl-POSS silsesquioxane cages, $Si_8O_{12}(CH_3)_8$ (gray solid lines), in nC_{16} at 400 K. For clarity, only the average values are reported. Statistical uncertainty for both data sets is similar to that reported in Figure 2.

The results obtained for bare and octamethyl-POSS show several marked differences. The first attractive peak between octafunctionalized silsesquioxanes is located at $r \cong 0.88$ nm, while it is located at $r \cong 0.75$ nm for bare silsesquioxanes. This shift to larger separations for the first attractive peak in the radial distribution function between octamethyl-POSS is expected because the methyl groups are bulkier than the hydrogen atoms; thus, the center-to-center distance corresponding to the first attractive peak has to be larger than that observed between bare silsesquioxanes in the same system. The first attractive peak in the radial distribution function is slightly less intense for octamethylsilsesquioxanes than it is for bare silsesquioxanes. This result probably indicates that $Si_8O_{12}(CH_3)_8$ monomers are more soluble in nC_{16} than $Si_8O_{12}H_8$ monomers are. We also note that the first attractive peak for octafunctionalized silsesquioxanes is significantly narrower compared to that between bare silsesquioxanes. More interestingly, the first attractive peak in the results shown in Figure 4 for octafunctionalized silsesquioxanes (gray solid line) is followed by a shoulder at $r \cong 1.05$ nm, and then the radial distribution function decreases monotonically to unity. Our results do not provide evidence for a midrange repulsion, even though some repulsion at $r \cong 1.35$ nm could be within the statistical uncertainty of the results here reported. In stark contrast, the results obtained for bare silsesquioxanes (black curve in Figure 4) indicate that a midrange repulsion is associated with the strong attraction.

To better appreciate the physical reasons beyond the features of both the radial distribution function and the potential of mean force discussed in Figure 4 between octafunctionalized POSS monomers in nC_{16}, we report in Figure 5 selected simulation snapshots for $Si_8O_{12}(CH_3)_8$ monomers dissolved in nC_{16} at 400 K. In the snapshots reported in Figure 5 we do not show the nC_{16} chains for clarity, and we only highlight two POSS monomers as they approach each other. The sequence of snapshots reported in Figure 5 suggests that as two POSS monomers approach they change their relative orientation. At relatively large center-to-center separations ($r \cong 1.25$ nm), a methyl group in the first POSS monomer points toward a methyl group in the second POSS monomer (corner-to-corner configuration). As the distance between the centers of mass decreases ($r \cong 1.15$ nm), a methyl group of the first POSS monomer points in the general direction of one oxygen atom in the second POSS monomer (corner-to-side configuration). At shorter separations ($r \cong 0.95$ nm), two methyl groups in the first POSS monomer slide in contact with the second POSS monomer (side-to-side configuration). Finally, in correspondence to the observed center-to-center separation of maximum attraction ($r \cong 0.88$ nm), we observe a configuration in which a methyl group of the first POSS monomer docks in the center of the face of the second POSS monomer (face-to-face configuration). The sequence of simulation snapshots reported in Figure 5 leads us to conclude that the rearrangement of the relative orientations between POSS monomers is responsible for the shoulder that follows the first peak in the radial distribution function presented in Figure 4.

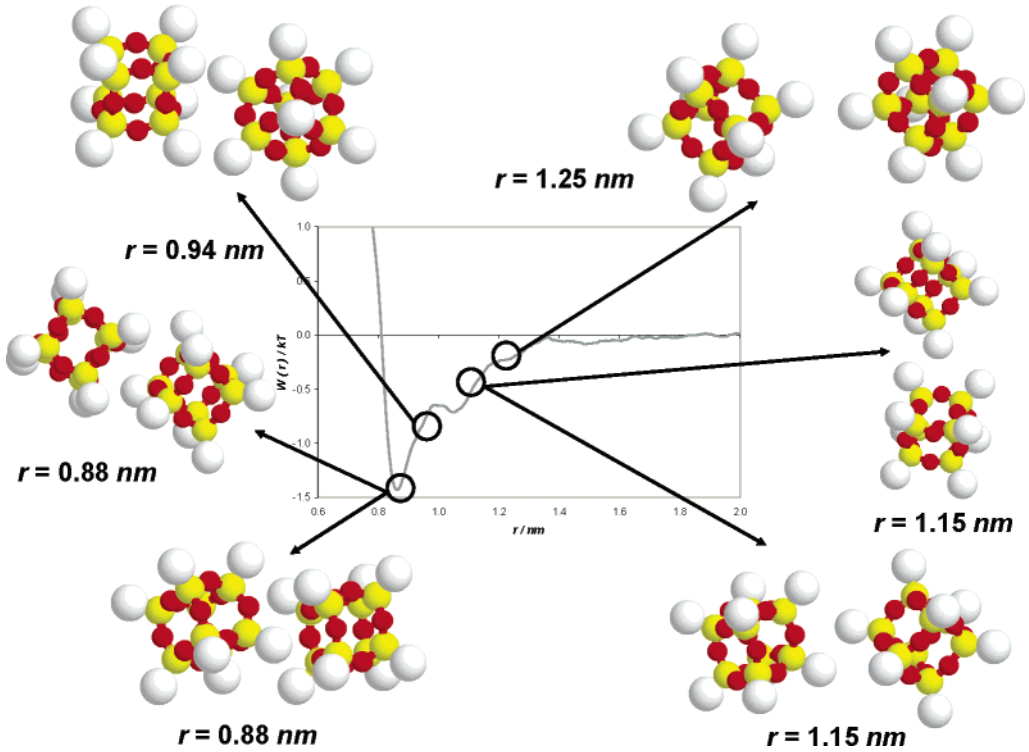

Figure 5. Sequence of simulation snapshots that reproduces the mechanism by which two octafunctionalized POSS monomers $[Si_8O_{12}(CH_3)_8]$ approach each other when they are dissolved in nC_{16} at 400 K. Yellow and red spheres represent silicon and oxygen atoms, respectively. White spheres represent methyl groups. The arrows indicate the effective pair potential of mean force that corresponds to each of the snapshots represented.

To appreciate the effect of the polymeric solvent on the features of effective POSS−POSS potential of mean force, we compare in Figure 6 the radial distribution function and potential of mean force (inset) between bare (Figure 6a) and octamethyl-POSS monomers (Figure 6b) dissolved either in nC_{16} (black solid lines) or in PDMS (gray solid lines) at $T = 400$ K (data for POSS in PDMS are taken from ref 20).

Several interesting differences can be observed. Let us focus on bare silsesquioxanes (Figure 6a). As discussed earlier (see Figure 2), results for the pair potential of mean force indicate an oscillatory behavior between attractive and repulsive regions in nC_{16} (black solid lines). When the bare silsesquioxanes are dissolved in PDMS, the effective pair potential of mean force is still oscillating between attractive and repulsive regions, but the oscillations are less frequent. We speculate that this different behavior is due to the fact that nC_{16} is a macromolecule whose building blocks are less bulky compared to those that constitute PDMS. Therefore, it is conceivable that nC_{16} monomers form structured layers between the interacting silsesquioxane monomers. These layers may be responsible for the oscillations observed in the effective pair potential. [We observe that the distance between two consecutive peaks, ~0.5 nm, is of the same order of magnitude of the Lennard-Jones size parameters used to describe Si−CH_3 and Si−CH_2 interactions (see Table 1).] Interestingly, the effective short-range attraction between pairs of bare silsesquioxanes is stronger in PDMS than in nC_{16}. This result is coupled with the observation that the midrange repulsion is stronger when bare silsesquioxanes are dissolved in nC_{16} than when they are dissolved in PDMS.

When octamethylsilsesquioxanes are considered (Figure 6b), the results obtained in the two solvents are very different. As mentioned earlier (see Figures 4 and 5), the radial distribution function and the effective pair potential of mean force between silsesquioxanes in nC_{16} (black solid lines) are characterized by a strong short-range attraction followed by a shoulder in the radial distribution function. The detailed analysis of simulation snapshots (see Figure 5) indicates that this behavior is due to the relative rearrangement of silsesquioxanes monomers as they approach each other. When the octamethylsilsesquioxanes are dissolved in PDMS, our results show a weak midrange repulsion that follows a significant short-range attraction. In addition, we note that the effective short-range attraction between the dissolved silsesquioxanes is stronger when they are dissolved in nC_{16} than when they are dissolved in PDMS. This latter result is probably due to the fact that octamethylsilsesquioxanes $[Si_8O_{12}(CH_3)_8]$ are chemically similar to PDMS; thus, they easily dissolve in it.

We now consider the effect of temperature on the radial distribution function and on the effective pair potentials of mean force between silsesquioxanes in nC_{16}. In Figures 7 and 8 we report the radial distribution function and the potential of mean force for bare and octamethyl-POSS monomers in nC_{16}, respectively, as a function of temperature. In analogy with our results for bare silsesquioxanes in PDMS,[20] the results reported in Figure 7 indicate that the radial distribution function between bare silsesquioxanes in nC_{16} does not depend appreciably on temperature. Our results indicate that by raising the temperature from 400 K (black solid lines) to 600 K (gray solid lines) and 1000 K (black dotted lines) the first attractive peak in the radial distribution function becomes slightly less intense, the first midrange repulsive peak becomes weaker, and the second attractive peak becomes less intense. While these results are expected because as the temperature increases the

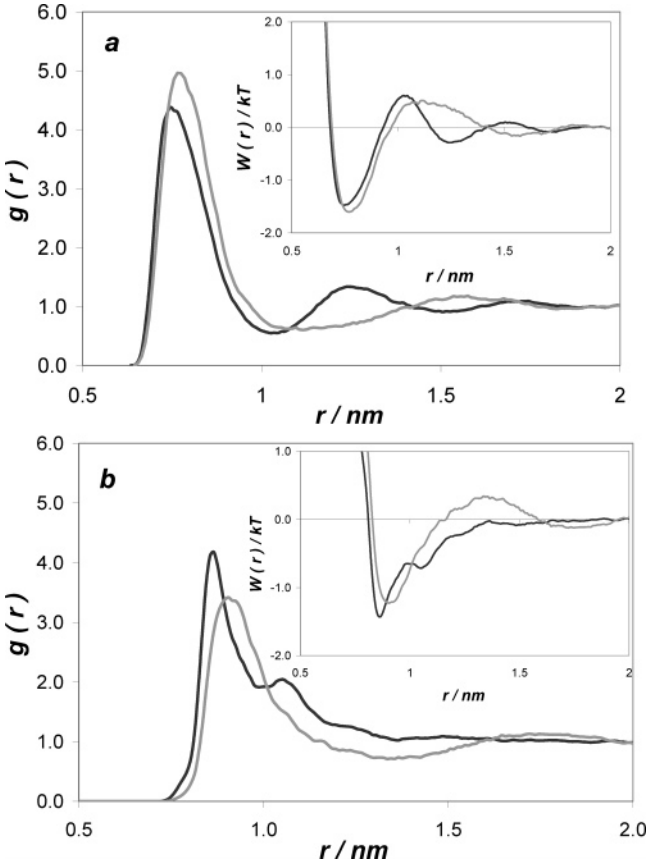

Figure 6. Radial distribution function and effective pair potential of mean force (inset) between bare silsesquioxanes [$Si_8O_{12}H_8$] (a) and between octamethyl-POSS [$Si_8O_{12}(CH_3)_8$] (b). Black solid lines are for results obtained for POSS monomers dissolved in nC_{16}. Gray solid lines are for results obtained for POSS monomers dissolved in PDMS. Results for POSS monomers in PDMS are from ref 20. Statistical uncertainties are not reported for clarity.

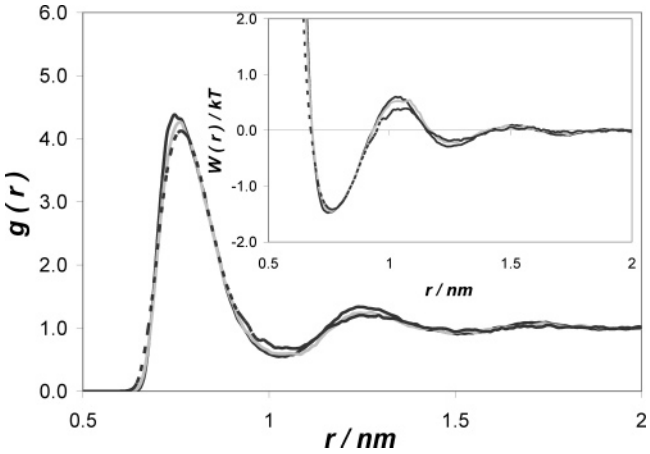

Figure 7. Radial distribution function and effective pair potential of mean force (inset) between bare POSS monomers, $Si_8O_{12}H_8$, dissolved in nC_{16} as a function of temperature. Black solid lines are for results obtained at $T = 400$ K. Gray solid lines are for results obtained at $T = 600$ K. Black dotted lines are for results obtained at $T = 1000$ K. Statistical uncertainties are not reported for clarity.

thermal fluctuations of the system increase, it should be noted that the listed differences are barely distinguishable when one considers the statistical uncertainty of our calculations. Because qualitatively similar results were obtained for bare silsesquioxanes dissolved in

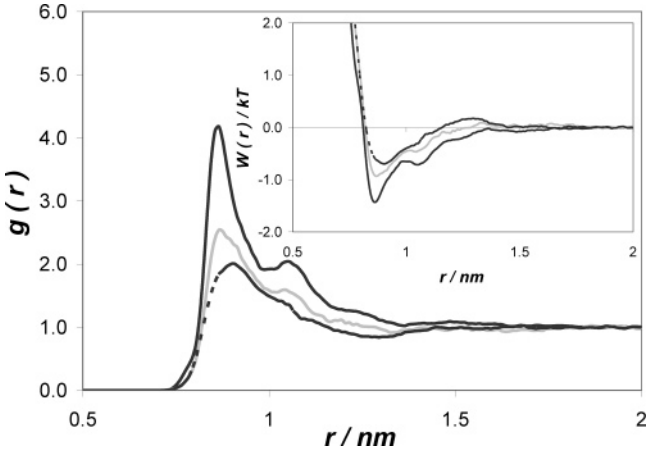

Figure 8. As in Figure 7, but for octamethyl-POSS [$Si_8O_{12}(CH_3)_8$] in nC_{16}.

PDMS,[20] we conclude that the effective attraction between bare silsesquioxane monomers dissolved in polymers may be too strong to be manipulated simply by adjusting the temperature (i.e., changing the temperature does not change the simulated $g(r)$ between bare POSS monomers in either nC_{16} or PDMS). This observation may have important technological implications in the manufacture of polymeric systems containing silsesquioxanes. In fact, this may be advantageous, as, for example, the clustering of carbon nanoparticles in synthetic rubber polymer is thought to impart strength to the nanocomposite.

In contrast with the results obtained for bare silsesquioxanes, the results reported in Figure 8 for the radial distribution function and effective pair potential of mean force between octamethylsilsesquioxane monomers [$Si_8O_{12}(CH_3)_8$] dissolved in nC_{16} show a pronounced dependence on temperature. The features of the radial distribution function obtained at 400 K (black solid lines) were discussed earlier in the text (see Figure 5). We note that the shoulder in both the radial distribution function and the effective pair potential of mean force becomes less pronounced as the temperature increases to 600 K (gray solid lines), and it eventually disappears at $T = 1000$ K (black dotted lines). We also note that as the temperature increases the first attractive peak in the radial distribution function becomes less intense and that a weak midrange repulsion, which is not clearly observed at low temperatures, is seen at $T = 1000$ K (black dotted lines). These observations reflect the expected behavior of the POSS−polymer systems because as the temperature increases the molecular thermal motion also increases, and the behavior of the dissolved silsesquioxanes becomes isotropic.

Osmotic Second Virial Coefficient. We report in Figure 9 the osmotic second virial coefficient calculated from numerical integration of eq 7 using the simulated results for the effective pair potentials of mean force. The data shown in Figure 9 will facilitate comparison between our simulations and experimental results. Unfortunately, however, we are not aware of experimental data that would allow such comparison. We report osmotic second virial coefficients B_{22} for POSS monomers in nC_{16} (Figure 9a) and in PDMS (Figure 9b) as a function of temperature. Data for the effective pair potential of mean force between POSS monomers in PDMS are from our earlier publication.[20] As shown in eq 7, the calculation of the osmotic second virial coef-

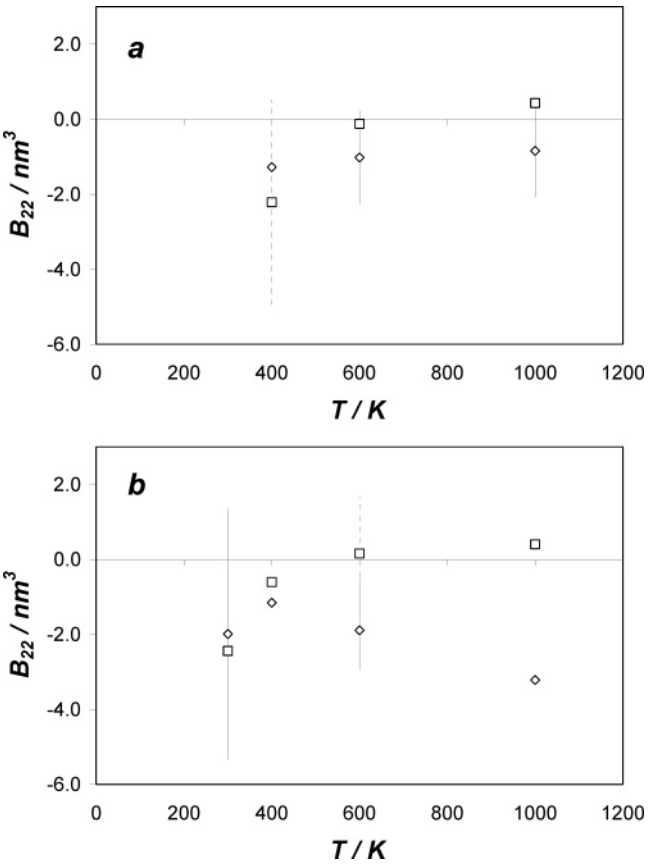

Figure 9. Osmotic second virial coefficient, B_{22}, computed from simulated pair potentials of mean force (see eq 7) as a function of temperature: (a) results obtained for POSS monomers dissolved in nC_{16}; (b) results obtained for POSS monomers dissolved in PDMS. In both panels, diamonds are for results obtained for bare POSS ($Si_8O_{12}H_8$) and squares are for results obtained for octamethyl-POSS [$Si_8O_{12}(CH_3)_8$]. Only representative statistical uncertainties are reported for clarity. The solid error bars refer to results for $Si_8O_{12}H_8$. The dashed error bars refer to results for $Si_8O_{12}(CH_3)_8$.

ficients B_{22} involves the integration of pair potentials of mean force as a function of the distance between the interacting molecules. As a consequence, small differences in the pair potentials of mean force may result in large differences in the computed osmotic second virial coefficients. Negative values for B_{22} provide macroscopic evidence for an effective attraction between molecules in solution, while positive values for B_{22} provide evidence for an effective repulsion between molecules in solution. A solvent is "good" for a specific solute when B_{22} is positive, and it is "poor" when the B_{22} is negative. It is in general possible to change the solvent quality by changing the temperature. In nonassociating systems B_{22} generally increases as the temperature increases; thus, a solvent could be "poor" at low temperatures and "good" at high temperatures. The temperature at which B_{22} equals zero is the theta temperature for that specific solvent−solute system.

Despite the large statistical uncertainties, several interesting features can be observed in the results shown in Figure 9. At low temperatures the osmotic second virial coefficient is predominantly negative for both $Si_8O_{12}H_8$ and $Si_8O_{12}(CH_3)_8$ in either nC_{16} (Figure 9a) or PDMS (Figure 9b), thus indicating an effective attraction between the silsesquioxanes. Interestingly, at low temperatures B_{22} is more negative for $Si_8O_{12}(CH_3)_8$ than it is for $Si_8O_{12}H_8$, thus indicating that octamethylsilsesquioxanes are effectively more strongly attracted to each other than bare silsesquioxanes are. This result is unexpected because the first attractive peak in the radial distribution function between octamethyl-POSS monomers in nC_{16} at 400 K is weaker than that between bare POSS monomers (see Figure 4). However, we note that the simulated potential of mean force between $Si_8O_{12}(CH_3)_8$ monomers in nC_{16} at 400 K does not show repulsive regions whereas that between $Si_8O_{12}H_8$ monomers does. As a consequence, the numerical integration of the potential of mean force by eq 7 yields an effectively stronger attraction between $Si_8O_{12}(CH_3)_8$ monomers than that between $Si_8O_{12}H_8$. This stronger attraction results in more negative values for B_{22}. Similar reasoning explains the difference observed for B_{22} between bare and octamethyl-POSS monomers at 300 K in PDMS.

As the temperature increases, B_{22} for $Si_8O_{12}H_8$ in both nC_{16} (diamonds in Figure 9a) and PDMS (diamonds in Figure 9b) remains negative. It is interesting to note that B_{22} for $Si_8O_{12}H_8$ in nC_{16} (diamonds in Figure 9a) increases very little as the temperature increases from 400 to 1000 K, while B_{22} for $Si_8O_{12}H_8$ in PDMS (diamonds in Figure 9b) increases slightly as the temperature increases from 300 to 400 K, but then decreases as the temperature increases from 400 to 1000 K. This behavior, typical for systems containing associating molecules,[31] is unexpected and may be an indication of strong association between bare silsesquioxanes in PDMS primarily due to solvent effects.

Results for B_{22} computed for $Si_8O_{12}(CH_3)_8$ in either nC_{16} (squares in Figure 9a) or PDMS (squares in Figure 9b) show the expected behavior for macromolecules dissolved in nonassociating solvents. The osmotic second virial coefficient is negative at low temperatures (indicating an effective attraction between the silsesquioxanes, thus characterizing the solvents as "poor") but becomes positive as the temperature increases (indicating an effective repulsion between the silsesquioxanes, thus characterizing the solvents as "good"). The theta temperature for $Si_8O_{12}(CH_3)_8$ is estimated via interpolation of the simulation results to be approximately 550 K in PDMS and 700 K in nC_{16}.

Self-Diffusion Coefficient. Our results for the mean-square displacement of the centers of mass of both bare and octamethyl-POSS in nC_{16} (data not shown for the sake of brevity) indicate that the mean-square displacement is a linear function of time; thus, it is possible to apply eq 8 to estimate the self-diffusion coefficients for silsesquioxanes in nC_{16}. In Figure 10 we report the self-diffusion coefficients for bare (diamonds) and octamethylsilsesquioxane monomers (squares) in nC_{16} as a function of temperature. In the inset of Figure 10 we report the logarithmic plot of the self-diffusion coefficients as a function of the inverse of the absolute temperature. We note that the self-diffusion coefficient for both bare and octamethylsilsesquioxanes increases as the temperature increases according to a functional dependence of the Arrhenius type:

$$D = D_0 \exp(-E_A/kT) \tag{9}$$

In eq 9, D_0 is a constant and E_A is the activation energy. Our best estimates for D_0 and E_A are reported in Table 2. Because of the low number of data sets, we do not attempt an evaluation of the statistical uncertainty on these results. Analysis of the individual trajectories did not show evidence of the hopping mechanism that

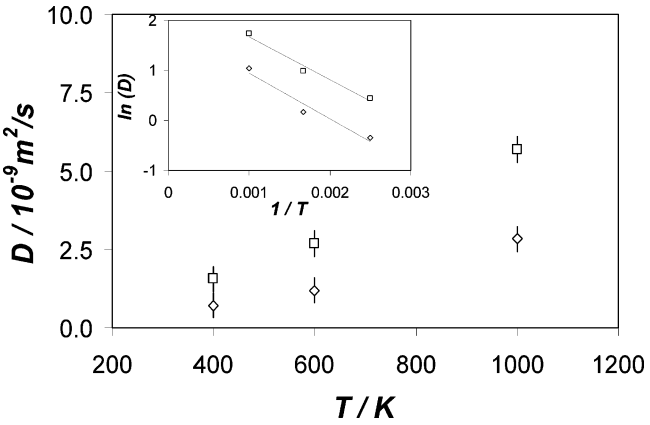

Figure 10. Self-diffusion coefficient for bare (squares) and octamethyl-POSS monomers (diamonds) dissolved in nC_{16} as a function of temperature. The inset is for the Arrhenius plot in which the natural logarithm of the self-diffusion coefficient is represented as a function of the inverse of the absolute temperature.

Table 2. Parameters D_0 and E_A Obtained by Fitting Eq 9 to the Diffusion Coefficient Data Shown in Figure 10

POSS	$\ln(D_0)$	E_A/k/K
$Si_8O_{12}H_8$	2.5	842
$Si_8O_{12}(CH_3)_8$	1.8	874

characterizes the diffusion of silsesquioxane monomers dissolved in PDMS.[20] To observe a hopping mechanism, it is required that small solute molecules are dissolved within a labyrinth of rigid polymer molecules.[32] The different diffusion mechanism is probably a consequence of the morphology of normal hexadecane, which is more flexible than PDMS, and therefore not able to trap the POSS cages in regions of low density within the polymeric matrix.

We also note that the simulated self-diffusion coefficients for silsesquioxanes in nC_{16} are slightly larger than those obtained in PDMS. This result is consistent with the different diffusive mechanism observed; the hopping mechanism in PDMS is presumably slower but could also be due to the higher viscosity of PDMS compared to that of nC_{16}. It is in fact expected that the diffusivity of a solute decreases as the viscosity of the solvent increases.

4. Summary

We have used canonical (*NVT*) molecular dynamics simulations to compute the thermodynamic and transport properties of polyhedral oligomeric silsesquioxane (POSS) monomers dissolved in normal hexadecane at 400, 600, and 1000 K. The POSS monomers considered are either bare (hydrogen-terminated) or octafunctionalized. In the octafunctionalized POSS monomers the hydrogen atoms of the bare POSS monomers are substituted by methyl groups.

We have reported molecular simulation data for the radial distribution function and for the effective potential of mean force between pairs of POSS monomers. Our simulations demonstrate that it is possible to tailor the effective POSS−POSS interactions by changing the system temperature and, more effectively, by substituting the hydrogen atoms in the bare silsesquioxane monomers with appropriate functional groups. The effective pair potentials of mean force are used to calculate the osmotic second virial coefficients for POSS monomers in normal hexadecane and in poly(dimethylsiloxane) as a function of temperature. The calculated osmotic second virial coefficients for $Si_8O_{12}H_8$ are negative both in normal hexadecane and in poly(dimethylsiloxane) at all temperatures considered, indicating that both solvents are "poor" for this silsesquioxane monomer. The calculated osmotic second virial coefficients for $Si_8O_{12}(CH_3)_8$ in both solvents are negative at low temperatures (below 500 K) but become positive as the temperature increases (above 600−700 K, depending on the solvent), suggesting that both solvents become "good" solvents at high temperatures. The theta temperature, the temperature at which the osmotic second virial coefficient equals zero, is approximately 550 K for octamethyl-POSS in poly(dimethylsiloxane) and 700 K for octamethyl-POSS in normal hexadecane. We also report self-diffusion coefficients evaluated for bare and octamethylsilsesquioxane monomers dissolved in normal hexadecane. Our results indicate that the self-diffusion coefficients increase as temperature increases, following a temperature dependence of the Arrhenius type.

Acknowledgment. The authors acknowledge financial support from the U.S. National Science Foundation under Contract DMR-0103399. Calculations were performed on the VAMPIRE cluster at Vanderbilt University.

References and Notes

(1) Giannelis, E. P. *Adv. Mater.* **1996**, *8*, 29.
(2) LeBaron, P. C.; Wang, Z.; Pinnavaia, T. *J. Appl. Clay Sci.* **1999**, *15*, 11.
(3) Tsagaropolous, G.; Eisenberg, A. *Macromolecules* **1995**, *28*, 6067.
(4) Paxton, J. P.; Mowles, E. D.; Eric, D.; Lukehart, C. M.; Witzig, A. J. *Proc. Am. Soc. Composites*, *16th Tech. Conf.* **2001**, 565.
(5) POSS is a trademark of Hybrid Plastics www.hybridplastics.com.
(6) Shockey, E. G.; Bolf, A. G.; Jones, P. F.; Schwab, J. J.; Chaffee, K. P.; Haddad, T. S.; Lichtenhan, J. D. *Appl. Organomet. Chem.* **1999**, *13*, 311.
(7) Cassagneau, T.; Caruso, F. *J. Am. Chem. Soc.* **2002**, *124*, 8172.
(8) Maka, K.; Itoh, H.; Chujo, Y. *Nano Lett.* **2002**, *2*, 1183.
(9) Kim, B.-S.; Mather, P. T. *Macromolecules* **2002**, *35*, 8378.
(10) Fu, B. X.; Yang, L.; Somani, R. H.; Zong, S. X.; Hsiao, B. S.; Phillips, S.; Blanski, R.; Ruth, P. *J. Polym. Sci., Part B: Polym. Phys.* **2001**, *39*, 2727.
(11) Kopesky, E. T.; Haddad, T. S.; Cohen, R. E.; Mckinley, G. H. *Macromolecules* **2004**, *37*, 8992.
(12) Pyun, J.; Matyjaszewski, K.; Wu, J.; Kim, G.-M.; Chun, S. B.; Mather, P. T. *Polymer* **2003**, *44*, 2739.
(13) Xu, H.; Kuo, J.-W.; Lee, J.-S.; Chang, F.-C. *Macromolecules* **2002**, *35*, 8788.
(14) Zheng, L.; Farris, R. J.; Coughlin, E. B. *Macromolecules* **2001**, *34*, 8034.
(15) Phillips, S. H.; Haddad, T. S.; Tomczak, S. J. *Curr. Opin. Solid State Mater. Sci.* **2004**, *8*, 21.
(16) Waddon, A. J.; Zheng, L.; Farris, R. J.; Coughlin, E. B. *Nano Lett.* **2002**, *2*, 1149.
(17) Choi, J.; Yee, A. F.; Laine, R. M. *Macromolecules* **2003**, *36*, 5666.
(18) Bharadwaj, R. K.; Berry, R. J.; Farmer, B. L. *Polymer* **2000**, *41*, 7209.
(19) Capaldi, F. M.; Rutledge, G. C.; Boyce, M. C. *Macromolecules* **2005**, *38*, 6700.
(20) Striolo, A.; McCabe, C.; Cummings, P. T. *J. Phys. Chem. B* **2005**, *109*, 14300.
(21) Watanabe, W.; Tsukagoshi, M.; Hirakoso, H.; Adschiri, T.; Arai, K. *AIChE J.* **2000**, *46*, 843.
(22) Frischknecht, A. L.; Curro, J. G. *Macromolecules* **2003**, *36*, 2122.
(23) Martin, M. G.; Siepmann, J. I. *J. Phys. Chem. B* **1998**, *102*, 2569.
(24) Ionescu, T. C.; Qi, F.; McCabe, C.; Striolo, A.; Kieffer, J.; Cummings, P. T. *J. Phys. Chem. B*, in press.

(25) Smith, W.; Forester, T. *J. Mol. Graph.* **1996**, *14*, 136.
(26) Allen, M. P.; Tildesley, D. J. *Computer Simulation of Liquids*; Oxford University Press: New York, 1987.
(27) Darden, T.; York, D.; Pedersen, L. *J. Chem. Phys.* **1993**, *98*, 10089.
(28) Striolo, A.; Colina, C. M.; Elvassore, N.; Gubbins, K. E.; Lue, L. *Mol. Simul.* **2004**, *30*, 437.
(29) Chandler, D. *Introduction to Modern Statistical Mechanics*; Oxford University Press: New York, 1987.
(30) Striolo, A.; Ward, J.; Prausnitz, J. M.; Parak, W. J.; Zanchet, D.; Gerion, D.; Milliron, D.; Alivisatos, A. P. *J. Phys. Chem. B* **2002**, *106*, 5500.
(31) Striolo, A.; Prausnitz, J. M. *Polymer* **2001**, *42*, 4773.
(32) Müller-Plathe, F.; Rogers, S. C.; van Gunsteren, W. F. *Chem. Phys. Lett.* **1992**, *199*, 237.

MA0512859